Title

PM2.5 exposure close to marijuana smoking and vaping: A case study in residential indoor and outdoor settings

Authors

Cheng, Kai-Chung
Ott, Wayne
Wallace, Lance
et al.

Publication Date

2022

DOI

10.1016/j.scitotenv.2021.149897

Peer reviewed

$PM_{2.5}$ Exposure Close to Marijuana Smoking and Vaping: a Case Study in Residential Indoor and Outdoor Settings

Kai-Chung Cheng,[1]* Wayne Ott,[1] Lance Wallace[2], Yifang Zhu[3], Lynn Hildemann[1]

[1]Stanford University, Stanford, CA; [2]Retired, Santa Rosa, CA; [3]University of California-Los Angeles, Los Angeles, CA

*corresponding author: kccheng@stanford.edu

ABSTRACT

We conducted 35 experiments for spatial measurement of marijuana aerosols in a current smoker's residential spaces. Fine particulate matter ($PM_{2.5}$) concentrations were measured every second at 1, 2, and 3 m horizontal distances from the smoker who performed prescribed 5-min smoking and vaping activities. In each experiment, five SidePak monitors measured $PM_{2.5}$ concentrations at five different angles facing the front of the smoker, representing the worst-case exposures. We studied the effect of distance from the smoker for two marijuana sources – smoking a marijuana cigarette, or *joint*, and vaping a liquid-cartridge vaping pen. Experiments were conducted in the family room indoors and in the backyard outdoors where the smoker normally consumes marijuana. Indoor marijuana vaping had higher average exposures (5-min $PM_{2.5}$) at 1 m distance than indoor marijuana smoking, but the levels from indoor vaping decreased more rapidly with distance (e.g., 77% reduction for vaping versus 33% for smoking from 1 to 2 m). Smoking and vaping in the outdoor environment reduce the

average exposures down to <5% of the indoor levels at each distance. Cumulative frequency distributions of the 1-s $PM_{2.5}$ concentrations revealed the frequencies of exceeding any selected transient peak exposure limit at a given distance. The frequency of exceedance decreased more quickly with distance for vaping than for smoking. Smoking and vaping outdoors made the transient peak exposures close to the source much less frequent than smoking and vaping indoors (e.g., <1% exceeded 1000 $\mu g/m^3$ outdoors versus >20% indoors at 1 m). Plotting the frequency of exceedance versus distance could offer additional guidance for a recommended minimum distance from a marijuana source.

INTRODUCTION

The District of Columbia and 15 States – Alaska, Arizona, California, Colorado, Illinois, Maine, Massachusetts, Michigan, Montana, Nevada, New Jersey, Oregon, South Dakota, Vermont, and Washington have legalized recreational marijuana use. As a result, involuntary exposure to secondhand marijuana smoke has become much more common in everyday settings across the country. Studies have shown that secondhand exposure close to tobacco smoking or vaping is substantially higher than farther away (e.g., Acevedo-Bolton et al, 2014; Ott et al, 2014; Nguyen et al, 2019) – this "*proximity effect*" will also be an issue near marijuana smoking or vaping.

The initial research investigating the proximity effect and spatial variation of exposure near a source used a tracer gas to mimic the transport of

emitted air pollutants. For example, McBride et al (1999) released carbon monoxide (CO) as a tracer in a residential living room while using 12 real-time CO monitors to measure concentrations at different indoor positions. Acevedo-Bolton et al (2012) deployed a larger monitoring array (30-37 CO monitors) in the same residential living room to characterize exposure as a function of the distance from a continuous CO source. Klepeis et al (2009) measured real-time CO concentrations at up to 36 points in a residential backyard to consider the proximity effect outdoors near a building. These tracer gas studies provided insight into how different environmental conditions (e.g., indoor ventilation or outdoor wind) influence the proximity effect; however, they did not account for the characteristics of real smoking or vaping emissions, such as the exhalation of mainstream smoke and the buoyancy of sidestream smoke that can also affect proximity exposure greatly.

Studies involving real human smoking or vaping were conducted mostly in prescribed settings. Acevedo-Bolton et al (2014) performed controlled experiments inside 2 homes (including a 158 m^3 living room) and 16 outdoor locations, using a small group of investigators wearing personal exposure monitors to measure $PM_{2.5}$ exposure close to prescribed tobacco cigarette smoking. Ott et al (2014) used a similar small-group monitoring approach to measure $PM_{2.5}$ exposure near prescribed tobacco cigarette smoking at 6 outdoor bus stops on California roadways. Zhao et al (2017) measured indoor $PM_{2.5}$ concentrations at 4 different distances from volunteers

performing e-cigarette vaping, using a standardized puff frequency (every 30 s) indoors in an 80 m^3 patient room in a clinical research center. Using a heated mannequin, Martuzevicius et al (2019) measured indoor particle exposures at 3 different distances from e-cigarette vaping, adopting the same 30 s puff frequency. Nguyen et al (2019) investigated particle concentrations at personal-space, social-space, public-space distances from non-prescribed vaping activities in California vaping shops. These studies provided valuable data for the levels of exposure close to tobacco smoking or vaping in real-world indoor and outdoor settings.

Marijuana is most often smoked in homes (Berg et al, 2015; Berg et al, 2018). Using a commercial real-time sensor (Dylos™ DC1700 monitor), a recent research study (Klepeis et al, 2017; Posis et al, 2019) monitored particle number concentrations in ~300 California residences. This study provided the first set of data on particle levels inside real homes with marijuana smoking. However, this large-scale study did not allow spatial measurement of exposure inside a home or accurate mass concentration measurements based on gravimetric calibration. Little is known about the $PM_{2.5}$ exposure close to a marijuana smoker. There also is virtually no knowledge of how different source types (smoking vs. vaping) and environments (indoor vs. outdoor) affect the proximity effect.

Our first goal was to examine, for the first time, $PM_{2.5}$ exposure close to a marijuana smoker and how the exposure can be reduced by increasing the distance from the source; we measured real-time $PM_{2.5}$ concentrations at 1,

2, and 3 m distances from marijuana emissions in a smoker's home and assessed both the level and frequency of exposure versus distance. Our second goal was to investigate whether choosing a different source type, a different location, or a different environmental setting can reduce the proximity exposure; we tested two common marijuana source types (the joint and the vaping pen) along with their corresponding exhalation patterns in an indoor and an outdoor location under different ventilation and air mixing conditions. Given the collected exposure data, an additional goal of our research was to explore data analysis methods that can potentially be useful for evaluating the recommended physical distance from marijuana sources to minimize involuntary exposure.

METHODOLOGY

Participant. A habitual user of marijuana (a 40-50 year old male) was recruited in this study. The cannabis materials were provided by the participant and consumed in his regular smoking spaces. The study protocol was accepted by the participant and approved by the Institutional Review Board at Stanford University.

Experimental Setup. We performed field research inside a residential property in San Jose, CA (Figure 1). This single-family home has two stories and a private backyard, and the marijuana smoker is the only occupant in this property. Five AM510 SidePak™ monitors (TSI, Shoreview, MN, USA) were deployed near the *indoor chair* in the 4.3×3.7×2.4 m (38 m^3) family

room or the *outdoor chair* in the backyard where the participant normally smokes or vapes marijuana (see the chairs marked with stars in Figure 1). Both chairs backed up to a wall, and the outdoor chair had a small table 0.7 m high to its immediate left. The 5 SidePak monitors were placed radially with 15° angle spacing at an equal distance from the source in each session (1 m, 2m, or 3m), measuring $PM_{2.5}$ concentration every 1 s; they were facing the front of the smoker to account for the worst-case exposure. Three monitors were placed at 1 m height (black circles), whereas two monitors were at 1.5 m height (white circles) to consider typical adult breathing heights while sitting and standing, respectively (Figure 1). The actual measured breathing heights of the smoker sitting on the indoor and outdoor chairs were 1.2 m and 1.1 m, respectively.

Using these monitoring settings, we performed 35 experiments (20 indoors and 15 outdoors). For the indoor experiments, 17 were performed with all windows and interior or exterior doors closed in the house – “base case” while 3 involved opening the family-room door (18” open) and two dining room windows (each 15” open) while running the fan of the centralized HVAC system (with one ceiling register in each room) – “alternative case”. For outdoor experiments, 12 were carried out with a fully-opened outdoor umbrella above the smoker (2 m height and 1.9 m in diameter) – “base case” – while 3 were carried out with this umbrella fully closed (<0.1 m in diameter) – “alternative case”. We hypothesize opening or closing the umbrella would noticeably affect the air mixing and proximity effect close to

the source. For the base-case experiments, all 5 monitors were underneath the umbrella when placed at 1 m distance from the smoker.

Air Velocity and Ventilation. We used the VelociCalc 8386 anemometer (TSI, Shoreview, MN, USA) to measure and log the indoor and outdoor air velocities near the smoking or vaping locations every 2 s during each experiment. This instrument has a 6-mm diameter sensor probe with a 25 mm long anemometer at its tip, and its minimum detectable air speed is 0.01 m/s. It was not possible to release carbon monoxide or sulfur hexafluoride tracer gas in the participant's house. As a way to estimate the magnitude of ventilation, we burned matches inside the house while using the Optical Particle Sizer 3330 (TSI, Shoreview, MN, USA) to measure the particle number concentrations every 1 min. The air change rate (ACH) was estimated by the log linear regression between concentration of the smallest particle size range (0.3-0.374 μm) and time after the well-mixed condition was reasonably achieved. Given the timescale of the experiments (1-2 h), diffusional and gravitational losses of particles within this size range were expected to be negligible compared with air exchange; this method has been used to estimate ACH in a residence where tracer gas releases were not feasible (e.g., Cheng et al 2020). These air change rate tests were performed outside the regular smoking or vaping experiments, because they involved particle emissions.

Sources and Protocol. We investigated two types of marijuana sources regularly used by the participant: (i) a cigarette-like marijuana joint (Caliva

“Toasties”) with 0% CBD and 9.6% THC, and (ii) an electronic vaping pen (AbsoluteXtracts, ABX) with the “Care by Design” 2:1 cartridge (CBD 46.1% and THC 21.9%). A standardized smoking or vaping protocol that consisted of 5 puffs over a 5-minute period was used. After inhaling, the participant exhaled at the starting point of every minute (black areas in Figure S1); we defined the 5 min period as the source period. This protocol was intended to enable comparisons between experiments with different source types or source distances based on the same exhalation or emission frequency (once every minute). Zhao et al (2017) and Martuzevicius et al (2019) have adopted this approach but with a different frequency (once every 30 s) for e-cigarette vaping. In our study, the participant chose the 1-min time interval for the 5-puff sequence to not exceed his normal habit of smoking and vaping. We did not choose a specific volume and duration for each puff, since we wanted to preserve the behavioral differences embedded in each puff for different source types (smoking versus vaping) and to investigate how they may affect the spatial variation of exposure close to a source.

The participant did not permit sensors to be used in contact with his body; therefore, puff topography or spirometry measurement involving sensor mouthpiece breathing was not conducted in this study. As a surrogate approach, we placed the VelociCalc anemometer in front of the smoker during the 5-min source period (Figure S1) at 0.1 m horizontal distance from the mouth position to record the “exhalation peak velocity” – the maximum air velocity produced by each exhalation (see Figure S2). This approach

enabled us to investigate human exhalation via air environment measurement. We discovered the temporal fluctuations of air velocities outdoors were comparable to the magnitudes of exhalation peak velocities. Therefore, we were not able to measure the exhalation peak velocities in the outdoor experiments. The durations of the exhalation were measured by the participant using a stopwatch. A test examining how consistently exhalation peak velocities can be produced and measured by the environmental sensing method is available in the Supplementary Material (Figure S3).

$PM_{2.5}$ Calibration. To ensure consistent measurements between monitors, we conducted a separate quality assurance study in which we placed 17 SidePak monitors (including the 5 monitors used in this study) inside a car chamber (2006 Honda Element) with a smoke source, simultaneously measuring $PM_{2.5}$ concentrations every 1 min. After the emission stopped and well-mixed condition was reasonably achieved (*gamma period*, Ott, 2007), the exponentially decaying measurements of the SidePak monitors were compared by linear regression with our reference SidePak monitor, giving $R^2 > 0.999$ for the 5 SidePak monitors used (forcing zero intercept). The slope of each linear regression (0.87-1.03) was used to rescale each measuring device to agree with the reference monitor.

The SidePak monitors measure $PM_{2.5}$ concentration based on light scattering properties, which are affected by the particle size and composition. To accurately represent the actual $PM_{2.5}$ concentration, the calibration factor (CF) – the ratio of gravimetrically-to-optically-measured

209 $PM_{2.5}$ concentration is needed for each source type (e.g., Jiang et al, 2011;
210 Dacunto et al, 2013). In a previously published paper, we determined the
211 CFs for the two marijuana source types: 0.35 for joint smoking and 0.44 for
212 vaping (Zhao et al, 2020) for the reference SidePak monitor; they were
213 applied along with the inter-monitor slopes to rescale all $PM_{2.5}$ measurement
214 in this study (e.g., actual concentration for vaping = direct reading of
215 $SidePak_i \times (0.44/[\text{slope of SidePak}]_i)$ where i = 1-5). Jiang et al (2011) found
216 that CFs for SidePak monitors remained relatively constant over time; for a
217 16-month period, the average difference was ~3%. The particle zero filter
218 was attached to the inlet of each SidePak monitor immediately before each
219 experiment for zero calibration.
220 **Decay and Mixing Characterization.** The $PM_{2.5}$ measurements at the 3
221 different distances (1 m, 2 m, and 3 m) were collected from separate
222 experiments, not simultaneously. It is important to ensure comparisons were
223 made based on comparable environmental settings. In each experiment,
224 therefore, we included a 5-min sampling period prior to the source period to
225 account for the variation in $PM_{2.5}$ background concentration. For each indoor
226 experiment, we added a 60-min sampling period following the source period
227 for determining the $PM_{2.5}$ decay inside the building. The decay rates were
228 determined by the log linear regressions between 1-min $PM_{2.5}$ concentrations
229 averaged over the 5 monitors (background subtracted) versus time during
230 the well-mixed decay periods. For the same source type (with the same
231 aerosol volatility), the $PM_{2.5}$ decay rate (the sum of the air change rate,

surface deposition rate, and evaporation loss rate) could reflect the relative strength of air mixing indoors. A higher air change rate will lead to stronger indoor air mixing (Drivas et al, 1996; Cheng et al, 2011), enhancing the particle surface deposition (e.g., Thatcher et al, 2002; He et al, 2005; Xiao et al, 2020). This suggests both the cause and consequence of stronger air mixing could contribute to a higher decay rate. Therefore, given a comparable evaporation loss rate (the same source type), a larger decay rate could indicate stronger air mixing indoors, which could cause more uniform concentration and a smaller proximity effect. Air mixing is one governing factor that affects the spatial distribution of concentration and exposure close to a source (e.g., Drescher et al, 1995; Cheng et al, 2011; Cheng et al, 2020). By examining the decay rates for experiments with the same source type, we can ensure comparisons are based on comparable air exchange and air mixing conditions.

RESULTS AND DISCUSSION

To determine the source and environmental characteristics in each indoor experiment, we calculated the average exhalation peak velocity and duration (averaged over 5 puffs) and the decay rate (from log-linear regression). Table 1 summarizes the statistics of average exhalation peak velocities, average exhalation durations, and decay rates for indoor smoking versus indoor vaping from 16-17 experiments with all the windows and doors closed without fan operating (ACH = 0.31-0.34 h^{-1}). These base-case experiments

had background air velocities below the anemometer's detection limit (<0.01 m/s) – this enabled more accurate determination of exhalation velocities for the two different sources. The mean of average exhalation peak velocities for indoor smoking (0.99 m/s) was ~2 times as high as that for indoor vaping (0.53 m/s). The mean of average exhalation durations for indoor smoking (2.3 s) was ~70% of that for indoor vaping (3.4 s). The mean decay rate for indoor vaping was higher than the mean decay rate for indoor smoking (0.75 versus 0.46 h^{-1}). Particle losses due to air exchange and particle settling are expected to be comparable for indoor smoking and vaping experiments; the sizable difference was likely due to the higher aerosol volatility for vaping. This finding was consistent with previous studies testing the decay rates of 4 different marijuana sources (joint, glass pipe, water pipe, and vaping pen) inside a car chamber (Zhao et al, 2020) and in a residential bedroom (Ott et al, 2020). Li et al (2020) found $PM_{2.5}$ particle loss rates for vaping aerosols (from e-cigarettes in this case) were >4 times as high as that for – Di-Ethyl-Hexyl-Sebacat (DEHS) aerosols with little evaporation. In addition to exhalation pattern, aerosol evaporation could have a significant effect on exposure versus distance from the source.

The average air velocities for outdoor experiments ranged from 0.21 to 0.33 m/s. The highest average velocity (0.33 m/s) was recorded when the overhead outdoor umbrella was folded (alternative case). This could be due in part to less blockage of the air movement. Klepeis et al (2009) and Acevedo-Bolton et al (2014) measured ground-level air velocities in the

backyard of a California home. Their reported average air velocities (0.26-0.34 m/s) were comparable to our measured values. These backyard measurements are expected to be affected by eddy currents near buildings.

Figures 2(a) and 2(b) show examples of the 1-s concentration time series of $PM_{2.5}$ measured indoors (top) and outdoors (bottom) at 1 m, 2 m, and 3 m horizontal distances from the participant performing marijuana vaping in the residential property (Figure 1). Unlike the standard indoor experiments that were performed separately with 1-h decay periods (see the Decay and Mixing Characterization section), continuous indoor measurements were taken across multiple source periods (grey areas) with only 5 minutes apart. This was to align with the emission sequence of the outdoor time series to allow comparisons between Figures 2(a) and 2(b). Here, all concentrations greater than the monitor's upper limit were replaced with 20 mg/m^3 (CF = 1), giving maximum concentrations ~10 mg/m^3 (CF = 0.44).

For both the indoor and outdoor experiments, the magnitudes and occurrences of transient concentration spikes – "*microplumes*" (e.g., Acevedo-Bolton et al, 2012; Cheng et al, 2014) – increased with decreasing distances, showing the proximity effect during active emissions (light grey regions in Figure 2). Striking differences were observed between indoor and outdoor situations. Microplumes were much more likely indoors than outdoors. In the indoor environment (without mechanical ventilation), aerosols could follow the exhaled airflow, moving toward the monitors that were in front of the vaper. In contrast, aerosol movement outdoors was

primarily governed by the wind patterns. The rapidly changing directionality of outdoor airflows near the building made microplumes less likely to emerge. The durations of microplumes were longer indoors than outdoors. The slower air movement indoors could make emitted plumes linger at a monitoring location. This effect can also be seen from the persistent $PM_{2.5}$ concentration time series after each source emission period ended indoors. As expected, the more frequent occurrences and longer durations of microplumes indoors greatly increased the average concentration and exposure at close proximity to the active emission source.

Figure 3 summarizes the time-averaged $PM_{2.5}$ concentrations over the 5-min source periods at 1, 2, and 3 m distances from the source in all the 35 indoor and outdoor experiments with marijuana smoking and vaping. Figures 3(a)-3(b) correspond to the condition with all windows and doors closed and without HVAC fan running (indoor base case) whereas Figure 3(c) involves opening a door and two windows and with HVAC fan running (indoor alternative case). Figures 3(d)-3(e) correspond to the condition with the umbrella open and above the smoker (outdoor base case) whereas Figure 3(f) involves fully closing the overhead umbrella (outdoor alternative case). Each boxplot contains measurements from the 5 SidePak monitors at different angles in front of the smoker (Figure 1) with the dashed line representing the mean value and the solid line representing the median. Background concentrations ranged from 1.2 to 6.8 $\mu g/m^3$; they were

subtracted from these 5-min $PM_{2.5}$ averages. Statistics of each boxplot are available in the Supplementary Material (Table S1).

The 5-min $PM_{2.5}$ concentrations at 1 m were higher and more variable for indoor vaping than for indoor smoking (mean = 1330 versus 870 $\mu g/m^3$; interquartile range = 1260 versus 670 $\mu g/m^3$; Figure 3(b) versus 3(a)). However, the levels of indoor vaping decreased more noticeably with distance than for indoor smoking (77% versus 33% reduction from 1 to 2 m and 63% versus 50% reduction from 2 to 3 m). This finding could be associated with the difference in exhalation pattern – the exhalation peak velocity for indoor vaping was only ~50% that of indoor smoking. Therefore, vaping aerosols are expected to have longer time for decay before reaching a given distance. Another consideration involves the aerosol evaporation process - the higher decay rate (>1.6 times higher) of the vaping aerosols due to their higher volatility could also result in a greater concentration decrease over distance.

The $PM_{2.5}$ exposures for indoor marijuana smoking (870 $\mu g/m^3$ at 1 m and 580 $\mu g/m^3$ at 2 m; Figure 3(a)) were much higher than for indoor tobacco smoking (320 $\mu g/m^3$ at 1.25 m and 60 $\mu g/m^3$ at 2 m; Acevedo-Bolton et al, 2014). This could be caused by the higher emission rate for marijuana smoking (7.8 mg/min versus 2.2 mg/min; Ott et al, 2020) accompanied with the smaller indoor volume (38 versus 158 m^3). Another factor was the different monitoring setups – our study used 5 monitors to cover 60° angle facing the smoker, making it more likely to capture the emitted plumes than

346 a single monitor. Similarly, $PM_{2.5}$ exposures for indoor marijuana vaping
347 (1330 $\mu g/m^3$ at 1 m and 310 $\mu g/m^3$ at 2 m; Figure 3(b)) were much higher
348 than indoor e-cigarette vaping (375 $\mu g/m^3$ at 0.8 m and 7 $\mu g/m^3$ at 2 m; Zhao
349 et al, 2017). This again was likely due to more monitors at each distance (5
350 versus 1) and the smaller indoor volume (38 versus 80 m^3). Both vaping
351 sources had a significant concentration decrease over distance, but the
352 marijuana decrease was smaller (77% versus 98%). This could be due in
353 part to the lower aerosol volatility of marijuana vaping compared to e-
354 cigarette vaping (Wallace et al, 2021).
355 Figure 3(c) shows the measurements from the only 3 indoor vaping
356 experiments (one for each distance) with the HVAC fan operating in the
357 house (alternative case). In addition to lowering the 5-min $PM_{2.5}$ levels (due
358 to increased aerosol removal), mechanical ventilation greatly reduced the
359 variation of the 5-min $PM_{2.5}$ averages measured at the 5 different angles at
360 each distance (Figure 3(c) versus 3(b)). In addition, it diminished the
361 pronounced concentration gradient over distance observed without
362 mechanical ventilation operating. As expected, stronger air mixing due to
363 mechanical ventilation made the $PM_{2.5}$ concentration more uniform in space.
364 The outdoor 5-min $PM_{2.5}$ levels at each distance were less than 5% of the
365 indoor levels for either smoking or vaping. Therefore, a different vertical
366 (concentration) scale was needed for Figures 3(d)-3(f). Again, the varied
367 airflow direction and more rapid plume movement outdoors made the $PM_{2.5}$
368 exposures in front of the smoker much lower than indoors. The $PM_{2.5}$

exposure for outdoor marijuana smoking (mean = 43 μg/m^3 at 1 m; Figure 3(d)) was higher than for outdoor tobacco smoking: 13 μg/m^3 at 1 m (Klepeis et al, 2007) and 29 μg/m^3 at 0.8-1.5 m (Acevedo-Bolton et al, 2014). In addition to the higher emission rate for marijuana smoking (Ott et al, 2020), use of 5 1-m monitors under an outdoor umbrella with the smoker made plume encounters more likely (see Figure 1). Most of the outdoor experiments involved the participant smoking or vaping under an outdoor umbrella (base case) except for the 3 alternative-case experiments in Figure 3(f) (one for each distance with 5 SidePak monitors). In these 3 experiments without an umbrella above the smoker, the lower exposures were likely caused by the less-enclosed setting. This, in combination with the highest recorded average air velocity (0.33 m/s), could cause greater dispersion of emitted particles near the smoker.

For each box plot in the 4 base-case graphs (Figures 3(a)-3(b) and Figures 3(d)-3(e)), we separated the 5-min averages into two groups based on 1 and 1.5 m breathing heights and calculated the mean for each group. For indoor vaping, the means of the 5-min averages for all the 3 distances (1 m, 2 m, and 3 m) were higher at 1 m than at 1.5 m height (Figure S4(b)). This is not surprising as the source was closer to 1 m height. In contrast, the means for all the 3 distances were higher at 1.5 m than at 1 m height for indoor smoking (Figure S4(a)). The difference was greatest at the shortest distance (1 m); the mean at 1.5 m height was ~1.7 times as high as the mean at 1 m height. This might be due to the stronger plume buoyancy created by a

392 combustion source – the burning joint – thus increasing the means at 1.5 m
393 height. The means of the 5-min averages outdoors (Figures S4(c)-4(d)) did
394 not necessarily follow the same pattern observed indoors; for outdoor
395 smoking (Figure S4(c)), the mean at the 1.5 m height was greater at 1 m
396 distance, but the outdoor means at 1 m height became greater at the 2 and
397 3 m distances. In the presence of outdoor wind, the effect of plume
398 buoyancy could become less noticeable, especially for greater distances
399 from the source.
400 Figures 4(a)-4(f) show the cumulative frequency distributions of 1-s $PM_{2.5}$
401 concentrations collected during 5-min source periods on log-probability
402 graphs for 18 indoor and outdoor experiments with smoking and vaping.
403 Again, the left four graphs corresponded to the base-case experiments
404 indoors (Figures 4(a)-4(b); with all windows and doors closed; without HVAC
405 fan running) and outdoors (Figures 4(d)-4(e)); outdoor umbrella open above
406 the smoker). The right two graphs (Figures 4(c) and 4(f)) corresponded to
407 the alternative-case experiments indoors (opening a door and two windows
408 and running the HVAC fan) and outdoors (folding the overhead umbrella),
409 respectively. Each frequency distribution contains aggregated
410 measurements from the 5 SidePak monitors at different angles (n = 1500).
411 Each graph compared the cumulative frequency distributions at 1, 2, and 3
412 m distances from the 3 experiments with similar environmental conditions.
413 Indoor experiments that had comparable decay rates were grouped together
414 for each graph: 0.34-0.37 h^{-1} for smoking (Figure 4(a)), 0.97-1.06 h^{-1} for

vaping (Figure 4(b)), and 6.9-7.8 h^{-1} for vaping with a door and two windows opened and HVAC fan running (Figure 4(c)) (see Methodology section for details). Experiments in each outdoor graph (Figures 4(d)-4(f)) were conducted consecutively with 5 min intervals to minimize the outdoor weather variation (e.g., Figure 2(b)). To avoid negative values for the log scale concentrations, the background concentrations (2-6.8 $\mu g/m^3$ indoors and 3.3-3.9 $\mu g/m^3$ outdoors) were included in these 1-s $PM_{2.5}$ concentration frequency distributions.

Plotting a cumulative frequency distribution on the log-probability graph, one can visualize the frequency of exceeding any given concentration limit. Taking figure 4(b) as an example, 10% of the concentrations exceeded 1000 $\mu g/m^3$ at 2 m from the source. The frequency increased to ~40% at 1 m and decreased to 0% at 3 m. For the same frequency of exceedance (10%), the concentration limit increased to ~4000 $\mu g/m^3$ at 1 m and decreased to ~150 $\mu g/m^3$ at 3 m.

Compared to indoor smoking (Figure 4(a)), the frequency distributions for indoor vaping (Figure 4(b)) showed much greater separation at the 3 distances. For example, from 1 to 3 m distance, the frequency of exceeding 1000 $\mu g/m^3$ dropped ~40% (from 38 to 0%) for indoor vaping but only ~10% (from 22 to 14%) for indoor smoking. The more noticeable decrease in the frequencies for vaping again could be associated with the longer travel time (due to lower breath exhalation peak velocity) and the higher decay rate compared to smoking. Turning on the mechanical ventilation system (Figure

4(c)) flattened the cumulative frequency distribution at each distance for the middle range of concentrations (50-500 $\mu g/m^3$). It also reduced the separation of the 3 frequency distributions. In addition to the average concentrations (5-min $PM_{2.5}$ in Figure 3(c)), the stronger mechanical air mixing made the transient concentrations (1-s $PM_{2.5}$) become more uniformly distributed in space.

Concentration peaks at each distance become much less likely to occur in the outdoor settings than indoors. For example, for both smoking (Figure 4(d)) and vaping (Figure 4(e)), less than 1% exceeded 1000 $\mu g/m^3$ at the 1 m distance outdoors compared to more than 20% indoors. At 2 and 3 m distances, 0% of the 1-second concentrations exceeded 1000 $\mu g/m^3$ outdoors while up to nearly 15% exceeded this level indoors. The separation of the frequency distributions at different distances occurs at a higher cumulative frequency range outdoors (50-70%; Figures 4(d)-4(e)) than indoors (5-10%; Figures 4(a)-4(b)). Folding the overhead outdoor umbrella reduced the peak concentrations at each distance; it also reduced the separation of the 3 cumulative frequency distributions (Figure 4(f) versus 4(e)). Like the indoor case (Figure 4(c) versus 4(b)), this could be caused by the stronger air mixing near the source due to a less enclosed environment, making the 1-s $PM_{2.5}$ concentrations more uniform in space. In this case, all the measured 1-s $PM_{2.5}$ concentrations dropped below 1000 $\mu g/m^3$ (0% frequency to exceed 1000 $\mu g/m^3$ for distances $\geq$ 1 m).

By obtaining cumulative frequency distributions of short-term concentrations at multiple distances, one can create a graph that shows how the frequency of exceedance varies with distance for a selected peak exposure limit. For example, using the 3 cumulative frequency distributions for outdoor smoking (Figure 4(d)), Figure (5) plotted frequency of exceedance versus distance for 3 selected peak exposure limits (50, 100, and 500 $\mu g/m^3$). A higher peak exposure limit (a less stringent limit) gave a lower frequency of exceedance at each distance. For each peak exposure limit, the frequency of exceedance decreased with increasing distance from the source. The decreases were more significant for a lower peak exposure limit (e.g., 50 $\mu g/m^3$), allowing the curves for the 3 limits to converge gradually. Assuming the case where <1% of exceedance is needed, keeping 1 m distance from the source could not meet any of the 3 peak exposure limits. Moving from 1 to 2 m distance, we could satisfy the least stringent peak exposure limit (500 $\mu g/m^3$). All the 3 peak exposure limits can be met if we moved further to the 3 m distance. The 24-h $PM_{2.5}$ standard offers a benchmark for assessment of long-term average exposures. The data analysis demonstrated here (Figures (4) and (5)) provides a possible standardized method to evaluate transient exposures to marijuana aerosols.

Limitations and Future Work. Optical sensor measurement could drift over time; it is optimal to calibrate optical monitors with the gravimetric shortly before the field experiments. Smoking and exhalation patterns vary across individuals; they could influence the concentration and spatial spread

of an emitted plume. For example, Fuoco et al (2014) and Zhao et al (2016) found particle concentration of e-cigarette vaping increased with puff duration; a higher exhalation velocity could increase the distance impacted by the emission. Future experiments examining how these behavioral patterns affect the proximity effect would be valuable. Particle size distribution influences the deposition of inhaled aerosols. Future research investigating the effect of distance on particle size distribution indoors and outdoors would be useful. This study shows how high PM2.5 levels could be inside a home with a marijuana smoker. PM2.5 has been associated with cardiorespiratory diseases; marijuana-related PM2.5 also has the potential to cause mental disorders. It is critical to examine the health effects of marijuana secondhand exposure for household members at home (e.g., children who live with marijuana smokers).

CONCLUSIONS

In summary, a clear proximity effect was observed for both smoking and vaping marijuana indoors without mechanical air mixing (HVAC fan running). A proximity effect was also evident outdoors when the participant smoked or vaped under a garden umbrella that limited air mixing. $PM_{2.5}$ exposures decreased more rapidly with distance from the source for vaping than for smoking, mostly likely caused by higher volatility of vaping aerosols. This finding suggests a smaller surrounding area of impact for vaping than for smoking. Smoking and vaping outdoors will reduce both average and transient peak exposures to exhaled aerosols. This is consistent with the

expectation that exposure to respiratory aerosols from a human source is less likely outdoors than indoors in light of the current COVID-19 pandemic. Previous measurements in Klepeis et al (2007) suggest outdoor exposure to tobacco smoke can be reduced noticeably when a person is ≥2 m away from the smoker. This is consistent with the results for outdoor marijuana smoking and vaping in this case study. With the legalization of recreational marijuana, cannabis smoking and vaping are rapidly emerging in everyday living environments. There is a critical need to address the question regarding the safe distance for marijuana smoking and vaping (e.g., can we apply the 12 ft safe distance for tobacco smoking to marijuana smoking?). This study was the first research systematically examining $PM_{2.5}$ exposure close to marijuana smoking and vaping in indoor and outdoor environment. The determination of the “concentration proximity curve” - average exposure versus the distance from the source could inform the safe distance policy or advisory. The characterization of the “frequency proximity curve” - frequency of peak exposure exceedance versus distance proposed here could provide additional insight into the related decision making. Results from a single marijuana smoker in a few indoor and outdoor locations cannot represent all possible exposure situations. Nonetheless, the initial proximity exposure measurements, findings, and data analysis methods presented here would be useful for the design of future field research investigating the proximity effect and safe distance for marijuana smoking and vaping.

ACKNOWLEDGEMENT

This research was supported by a grant (Award# 28IR-0062) from the Tobacco-Related Disease Research Program (TRDRP, Oakland, CA).

REFERENCES

Acevedo-Bolton, V., Cheng, K.C., Jiang, R.T., Ott, W.R., Klepeis N.E., Hildemann L.M., 2012. Measurement of the proximity effect for indoor air pollutant sources in two homes. *Journal of Environmental Monitoring*, 14, 94-104.

Acevedo-Bolton, V., Ott, W.R., Cheng, K.C., Jiang, R.T., Klepeis N.E., Hildemann L.M., 2014. Controlled experiments measuring personal exposure to PM2.5 in close proximity to cigarette smoking. *Indoor Air*, 24, 199-212.

Berg, C.J., Buller, D.B., Schauer, G.L., Windle, M., Stratton, E., Kegler, M.C., 2015. Rules regarding marijuana and its use in personal residences: findings from marijuana users and nonusers recruited through social media, *Journal of Environmental and Public Health* ID 476017. http//dx.doi.org/10.1155/2015/476017. Accessed on January 19, 2021.

Berg, C.J., Haardörfer, R., Wagener, T.L., Kegler, M.C., Windle, M., 2018. Correlates of allowing tobacco product or marijuana use in the homes of

young adults, *Pediatrics* 2018:141:S10. https://doi: 10.1542/peds.2017-1026E. Accessed on January 9, 2021.

Cheng, K.C., Acevedo-Bolton, V., Jiang, R.T., Klepeis, N.E., Ott, W.R., Fringer, O.B., and Hildemann, L.M., 2011. Modeling exposure close to air pollution sources in naturally ventilated residences: Association of turbulent diffusion coefficient with air change rate. *Environmental Science and Technology*, 45, 4016-4022.

Cheng, K.C., Acevedo-Bolton, V., Jiang, R.T., Klepeis, N.E., Ott, W.R., Kitanidis, P.K., Hildemann, L.M., 2014. Stochastic modeling of short-term exposure close to an air pollution source in a naturally ventilated room: An autocorrelated random walk method. *Journal of Exposure Science and Environmental Epidemiology*, 24, 311-318.

Cheng, K.C., Zheng, D., Hildemann, L.M., 2020. Impact of fan mixing on air pollutant exposure near indoor sources: an analytical model to connect proximity effect with energy. *Building and Environment*, 183, 107185. https://doi.org/10.1016/j.buildenv.2020.107185 Accessd on January 27, 2021.

Dacunto, P.J., Cheng, K.C., Acevedo-Bolton, V., Jiang, R.T., Klepeis, N.E., Repace, J.L., Ott, W.R., Hildemann, L.M., 2013. Real-time particle monitor

calibration factors and PM2.5 emission factors for multiple indoor sources. *Environmental Science Processes & Impacts*, 15, 1511-1519.

Drescher, A.C., Losbascio, C., Gadgil, A.J., Nazaroff, W.W., 1995. Mixing of a point-source indoor pollutant by forced convection. *Indoor Air*, 5, 204-214.

Drivas, P.J., Valberg, P.A., Murphy, B.L., Wilson, R., 1996. Modeling indoor air exposure from short-term point source releases. *Indoor Air*, 6, 271-277.

Fuoco, F.C., Buonanno, G., Stabile, L., Vigo, P., 2014. Influential parameters on particle concentration and size distribution in the mainstream of e-cigarettes. Environmental Pollution, 184, 523-529.

He, C., Morawska, L., Gilbert, D., 2005. Particle deposition rates in residential houses. *Atmospheric Environment*, 39, 3891-3899.

Jiang, R.T., Acevedo-Bolton, V., Cheng, K.C., Klepeis N.E., Ott, W.R., and Hildemann L.M., 2011. Determination of response of real-time SidePak AM510 monitor to secondhand smoke, other common indoor aerosols, and outdoor aerosol. *Journal of Environmental Monitoring*, 13, 1695-1702.

Klepeis, N.E., Bellettiere, J., Hughes, S.C., Nguyen, B., Beradi, V., Liles, S., Obayashi, S., Hofstetter, C.R., Blumberg, E., Hovell, M.F., 2017. Fine particles

in homes of predominantly low income families with children and smokers: Key physical and behavioral determinants to inform indoor-air-quality interventions, *PLoS ONE* 12(5).e017718. https://doi.org/10.1371/journal.pone.0177718 Accessd on January 19, 2021.

Klepeis, N.E., Gabel, E.B., Ott, W.R., Switzer, P., 2009. Outdoor air pollution in close proximity to a continuous point source. *Atmospheric Environment*, 43, 3155-3167.

Klepeis, N.E., Ott, W.R., Switzer, P., 2007. Real-time measurement of outdoor tobacco smoke particles. *Journal of the Air & Waste Management Association*, 57, 522-534.

Li, L, Lee, E.S., Nguyen, C., Zhu, Y, 2020. Effect of propylene glycol, vegetable glycerin, and nicotine on emissions and dynamics of electronic cigarette aerosols. *Aerosol Science and Technology*, 54, 1270-1281.

Martuzevicius, D., Prasauskas, T., Setyan, A., O'Connell, G., Cahours, X., Julien, R., Colard, S., 2019. Characterization of the spatial and temporal dispersion differences between exhaled e-cigarette mist and cigarette smoke. *Nicotine & Tobacco Research*, 21, 1371-1377.

McBride, S.J., Ferro, A., Ott, W.R., Switzer, P., Hildemann, L.M., 1999. Investigations of the proximity effect for pollutants in the indoor environment. *Journal of Exposure Analysis and Environmental Epidemiology*, 9, 602-621.

Nguyen, C. Li, L., Sen, C. A., Ronquillo, E., Zhu, Y., 2019. Fine and ultrafine particles concentrations in vape shops. *Atmospheric Environment*, 211, 159-169.

Ott, W., Mathematical modeling of indoor air quality. In: *Exposure Analysis*. Ott, W., Steinemann, A., Wallace, L. Eds.; Taylor & Francis Group: Boca Raton, FL, 2007.

Ott, W.R., Acevedo-Bolton, V., Cheng, K.C., Jiang, R.T., Klepeis, N.E., Hildemann, L.M., 2014. Outdoor fine and ultrafine particle measurements at six bus stops with smoking on two California arterial highways -- Results of a pilot study. *Journal of the Air and Waste Management Association*, 64, 47-60.

Ott, W.R., Zhao, T., Cheng, K.C., Wallace, L.A., Hildemann, L.M., 2020. Measuring indoor fine particle concentrations, emission rates, and decay rates from cannabis use in a residence (sumitted to *Atmospheric Environment: X*).

Posis, A., Bellettiere, J., Liles, S., Alcaraz, J., Nguyen, B., Berardi, V., Klepeis, N.E., Hughes, S.C., Wu, T., Hovell, M.F., 2019. Indoor cannabis smoke and children's health. *Preventive Medicine Reports*, 14, 100853. https://doi.org/10.1016/j.pmedr.2019.100853 Accessed on January 24, 2021.

Thatcher, T.L., Lai, A.C.K., Moreno-Jackson, R., Sextro, R.G., Nazaroff, W.W., 2002. Effects of room furnishings and air speed on particle deposition rates indoors. *Atmospheric Environment*, 36, 1811-1819.

Wallace, L.A., Ott, W.R., Cheng, K.C., Zhao, T., Hildemann, L.M., 2021. Method for estimating the volatility of aerosols using the Piezobalance: Examples from vaping e-cigarette and marijuana liquids. Atmospheric Environment, 253, 118379. https://doi.org/10.1016/j.atmosenv.2021.118379

Xiao, Y., Lv, Y., Zhou, Y., Liu, H., Liu, J., 2020. Size-resolved surface deposition and coagulation of indoor particles. International Journal of Environmental Health Research, 30, 251-267.

Zhao, T., Shu, S., Guo, Q., Zhu, Y., 2016. Effects of design parameters and puff topography on heating coil temperature and mainstream aerosols in electronic cigarettes. Atmospheric Environment, 134, 61-69.

Zhao, T., Nguyen, C., Lin, C.H., Middlekauff, H.R., Peters, K., Moheimani, R., Guo, Q, Zhu, Y., 2017. Characteristics of secondhand electronic cigarette aerosols from active human use. Aerosol Science and Technology, 51, 1368-1376.

Zhao, T., Cheng, K.C., Ott, W.R., Wallace, L., Hildemann, L.M., 2020. Characteristics of secondhand cannabis smoke from common smoking methods: calibration factor, emission rate, and particle removal rate. *Atmospheric Environment* https://doi.org/10.1016/j.atmosenv.2020.117731 Accessed on January 24, 2021.

Table 1. Comparison of average exhalation peak velocity, average exhalation duration, and decay rate between marijuana smoking versus vaping for base-case indoor experiments (all the windows/doors closed without fan operating).

	Average exhalation peak velocity[a] (m/s)	**Average exhalation duration[b] (s)**	**Decay Rate (1/h)**
Smoking	$n = 8$	$n = 8$	$n = 8$
Mean (IQR)[c]	0.99 (0.61)	2.30 (0.35)	0.46 (0.19)
Vaping	$n = 8$[d]	$n = 8$[d]	$n = 9$
Mean (IQR)[c]	0.53 (0.34)	3.43 (1.00)	0.75 (0.55)

[a] Exhalation peak velocity averaged over 5 puffs in each experiment
[b] Exhalation duration averaged over 5 puffs in each experiment
[c] Interquartile range (difference between 75th and 25th percentiles)
[d] Did not take the measurement in 1 of the 9 vaping experiments

Figure 1. Indoor and outdoor monitoring setups in participant's house. SidePak monitors (black and white circles) were facing the front of the smoker (star) sitting either on the chair in the family room or the chair in the backyard under the outdoor umbrella.

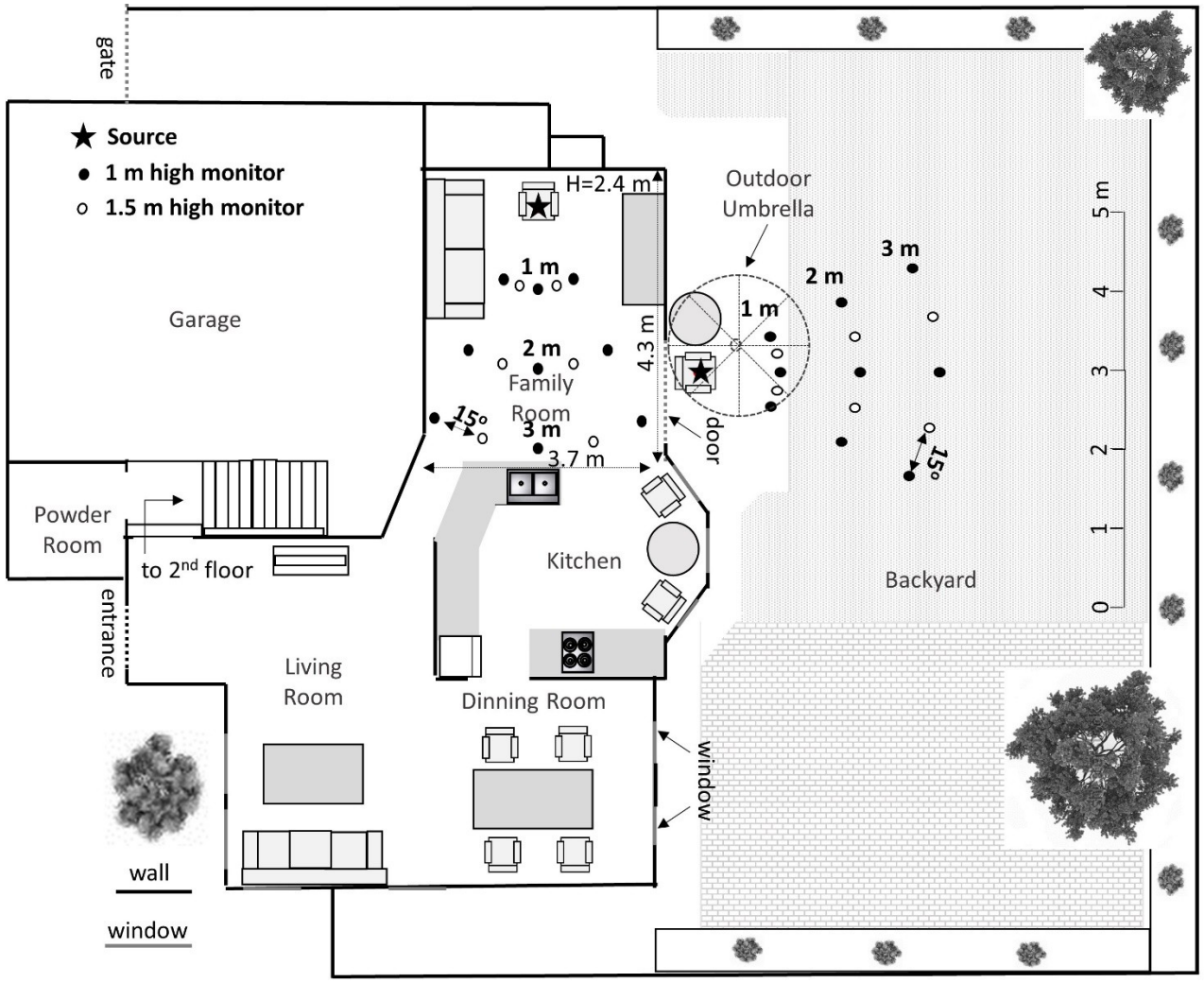

Figure 2. Example time series of 1-s $PM_{2.5}$ concentrations measured (a) indoors and (b) outdoors by 5 SidePak monitors (#1, #2, #3, #4, #5) at 1, 2, and 3 m distances from marijuana vaping. In each time series, monitors were moved between different distances between successive source periods (grey areas).

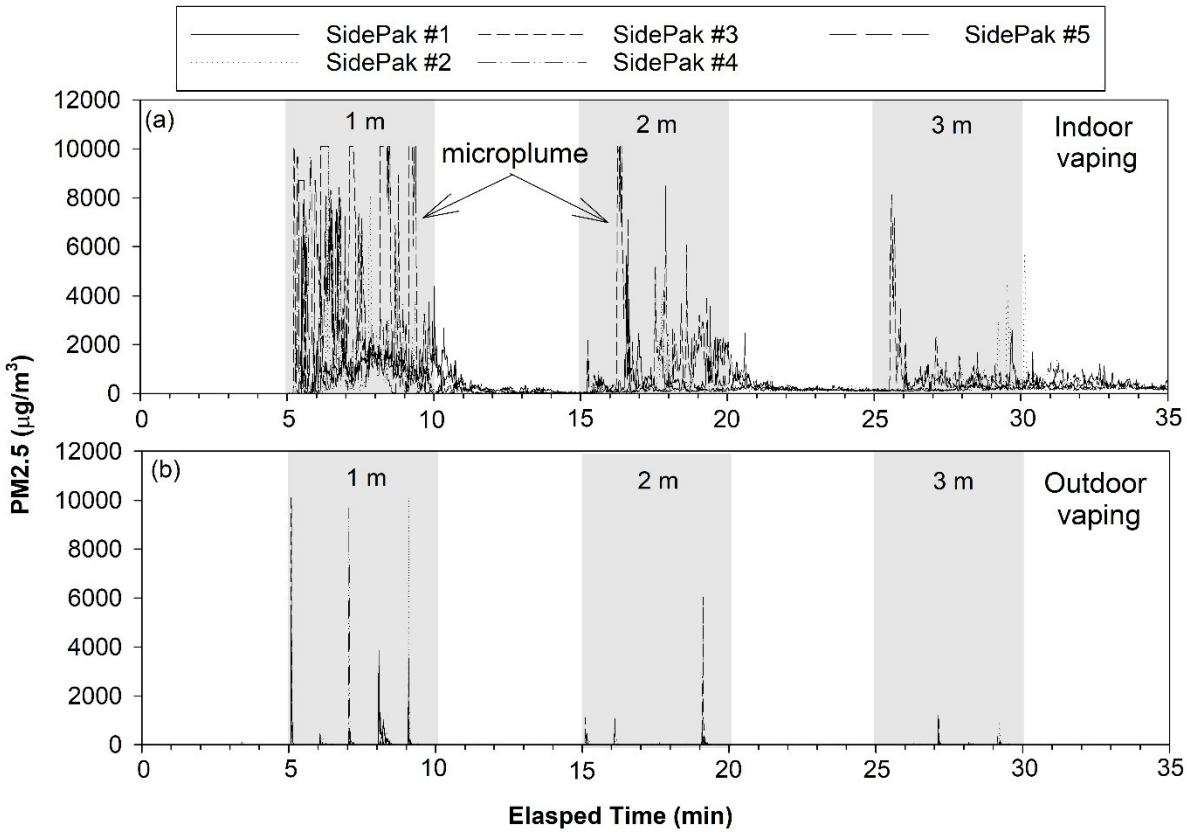

Figure 3. 5-min $PM_{2.5}$ exposures at 1, 2, and 3 m distances from the source for (a) indoor smoking with all windows and doors closed and HVAC off (base case), (b) indoor vaping with all windows and doors closed and HVAC off (base case), (c) indoor vaping with the HVAC fan operating and 1 door and 2 windows opened (alternative case), (d) outdoor smoking with the outdoor umbrella above the smoker opened (base case), (e) outdoor vaping with the outdoor umbrella above the smoker opened (base case), and (f) outdoor vaping with the overhead outdoor umbrella folded (alternative case). The boxes are the 25th and 75th percentiles; the whiskers are the 10th and 90th percentiles; the dots are outliers. The dashed lines are the means and the solid lines are the medians.

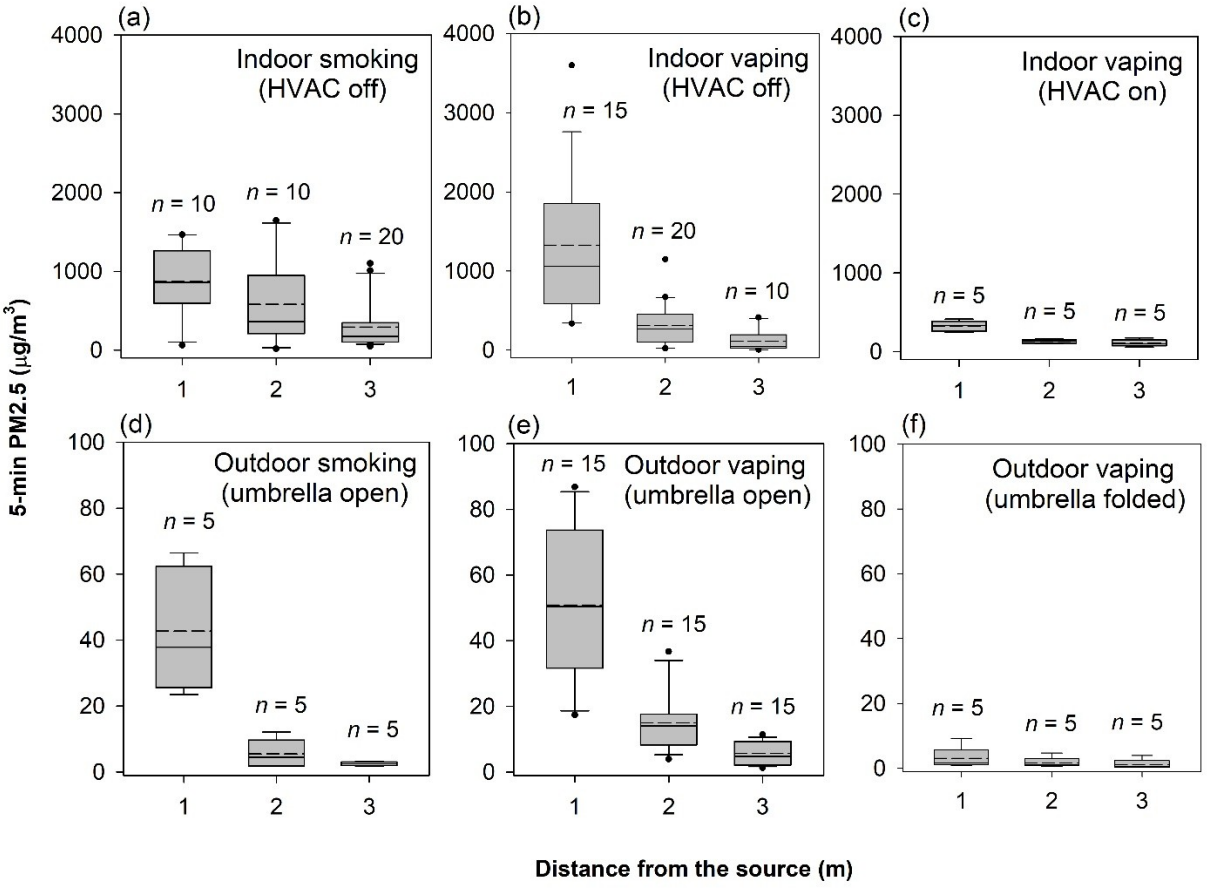
(a)
Indoor smoking
(HVAC off)
n = 10
n = 10
n = 20
(b)
Indoor vaping
(HVAC off)
n = 15
n = 20
n = 10
(c)
Indoor vaping
(HVAC on)
n = 5
n = 5
n = 5
(d)
Outdoor smoking
(umbrella open)
n = 5
n = 5
n = 5
(e)
Outdoor vaping
(umbrella open)
n = 15
n = 15
n = 15
(f)
Outdoor vaping
(umbrella folded)
n = 5
n = 5
n = 5
5-min PM2.5 (μg/m3)
Distance from the source (m)

718

719

Figure 4. Cumulative frequency distributions of 1-s $PM_{2.5}$ concentrations at 1, 2, 3 m distances from the source on log-probability graphs for (a) indoor smoking with all windows and doors closed and HVAC off (base case), (b) indoor vaping with all windows and doors closed and HVAC off (base case), (c) indoor vaping with the HVAC fan operating and 1 door and 2 windows opened (alternative case), (d) outdoor smoking with the outdoor umbrella above the smoker opened (base case), (e) outdoor vaping with the outdoor umbrella above the smoker opened (base case), and (f) outdoor vaping with the overhead outdoor umbrella folded (alternative case).

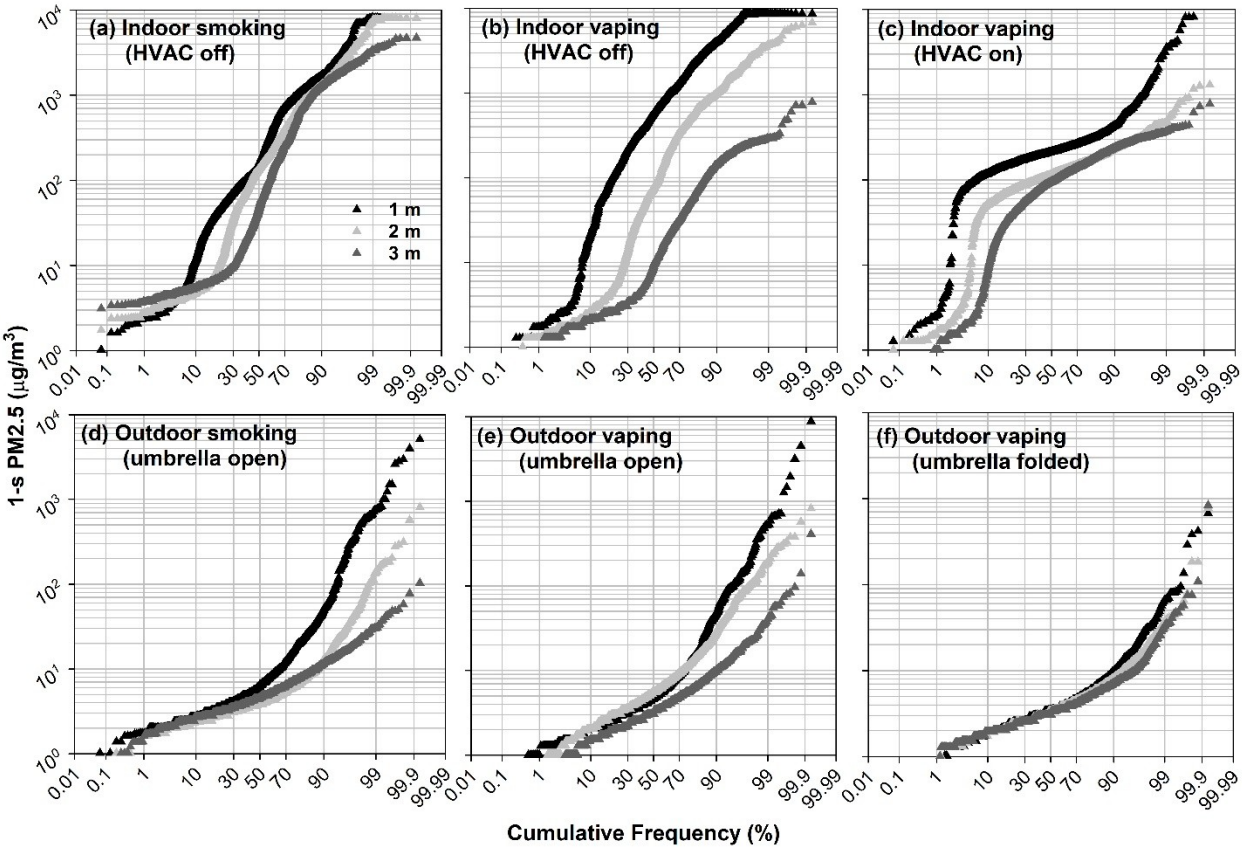

731

Figure 5. Example plot showing frequencies of exceeding 3 transient exposure limits (50, 100, 500 μg/m^3) at 1, 2, and 3 m distances from the source for outdoor smoking (based on data from Figure 4(d)).